NeuroImage: Clinical 24 (2019) 102038

Contents lists available at ScienceDirect

NeuroImage: Clinical

journal homepage: www.elsevier.com/locate/ynicl

fMRI functional connectivity as an indicator of interictal epileptic discharges

Su Jianpo[a,b,*], Khoo Hui Ming[c], Nicolás von Ellenrieder[a], Zeng Ling-Li[b], Hu Dewen[b], François Dubeau[a], Jean Gotman[a]

[a] Montreal Neurological Institute and Hospital, McGill University, Montreal, Canada
[b] College of Intelligence Science and Technology, National University of Defense Technology, Changsha, Hunan, China
[c] Department of Neurosurgery, Osaka University Graduate School of Medicine, Suita, Japan

ARTICLE INFO

Keywords:
IED
EEG/fMRI
Maximal BOLD response
Functional connectivity
Intracranial EEG

ABSTRACT

Objective: To explore the relationship between functional connectivity and presence of interictal epileptic discharges (IEDs) in different brain regions in intracranial EEG (iEEG).

Methods: We studied 38 focal epilepsy patients who underwent simultaneous EEG/fMRI scanning and subsequent intracerebral stereo-EEG investigation. In EEG/fMRI analysis, IEDs with different spatial distributions were considered independent studies and IED-related maximal BOLD responses were evaluated. Studies with iEEG electrodes inside the maximal responses were selected and divided into three groups: Studies with 1. distinct maximal BOLD highly concordant with seizure-onset-zone (SOZ); 2. Moderate maximal BOLD concordant with SOZ; 3. maximal BOLD discordant with SOZ. Using maximal BOLD as seed, its functionally connected zone (FCZ) was determined. IED rates in iEEG channels inside and outside the FCZ were compared in the three groups. The effect of laterality and distance between channels and maximal BOLD, and correlation between functional connectivity values and IED rates were analyzed.

Results: Thirty-six studies in 25 patients were included. IED rates of intracranial EEG channels inside the FCZ were significantly higher than outside in Group 1 ($p = 2.6 \times 10^{-6}$) and Group 2 ($p = 1.2 \times 10^{-3}$) and the inside-outside difference remained after regressing distance and laterality factors. In Group 1, connectivity values were significantly correlated with IED rates in channels inside the FCZ ($p < 0.05$).

Significance: Our results indicate a higher probability of finding intracranial IEDs in the FCZ of SOZ-concordant maximal BOLD responses than in other regions, regardless of distance and laterality. In studies with distinct maximal BOLD, connectivity values can partially predict IED rates in intracranial EEG. It is thus feasible to non-invasively delineate brain regions that are likely to have high IED rates.

1. Introduction

Interictal epileptic discharges (IEDs) are closely related to seizures (Chauvière et al., 2012; Staley et al., 2005; Staley et al., 2011). The maximal hemodynamic response to scalp IEDs in EEG/fMRI studies localizes with high probability the seizure-onset-zone (SOZ) (Khoo et al., 2017) and the spike-onset-zone (Khoo et al., 2018) in focal epilepsy. Resection of this region indicates a good outcome (Coutin-Churchman et al., 2012; Greiner et al., 2016; An et al., 2013). However, seizures may remain in some cases (Marsh et al., 2010), which calls for research into the generation and propagation of IEDs and seizures.

Studying the propagation of IEDs is important to understand epileptic networks (Sabolek et al., 2012; Smith and Schevon, 2016) and aid in intracerebral EEG (iEEG) implantation planning. High synchrony of intracerebral IED activity was found between regions inside widespread hemodynamic responses in EEG/fMRI studies (Khoo et al., 2017). Other multimodal analyses, however, revealed that measures of functional connectivity by iEEG and BOLD signals give complementary but sometimes inconsistent information (Bettus et al., 2011). Intrinsic and task-dependent coupling was found between iEEG and fMRI connectivity (Foster Brett et al., 2015; Kucyi et al., 2018), indicating that the two modalities often provide parallel connectivity information. Therefore, as fMRI-based functional network relates to the iEEG network during the interictal period, the fMRI functional network based in IEDs may predict IED emergence in iEEG.

We hypothesize that fMRI-based connectivity may indicate non-invasively the presence of IEDs observed in iEEG. In patients with focal epilepsy, we used EEG/fMRI to locate the maximal BOLD response to scalp IEDs. Taking the peak voxel as seed, a functionally connected zone (FCZ) was defined. IED rates in iEEG channels inside and outside the

* Corresponding author.
E-mail address: jianpo.su@mail.mcgill.ca (J. Su).

https://doi.org/10.1016/j.nicl.2019.102038
Received 5 August 2019; Received in revised form 2 October 2019; Accepted 15 October 2019
Available online 23 October 2019

FCZ were compared to determine whether IEDs are more probable inside this zone. If so, it becomes possible to define non-invasively brain regions where IEDs are likely to be present.

2. Methods

2.1. Subjects

Among the patients who participated in EEG/fMRI procedures between April 2006 and 2015, we identified 38 subjects with drug-resistant focal epilepsy who had a statistically significant BOLD response and also underwent stereo-EEG (SEEG) implantation for surgical evaluation. The implantation was performed independently of the experimental EEG/fMRI procedure and occurred usually a few months later.

2.2. Standard protocol approvals, registrations, and patient consents

Written informed consent for the EEG/fMRI procedure was obtained from each patient and the research was approved by the Research Ethics Committee of the Montreal Neurological Institute and Hospital.

2.3. EEG/fMRI acquisition and analysis

EEG/fMRI acquisition and analysis were performed as in previous studies (An et al., 2013; Moeller et al., 2009; Pittau et al., 2013). The detailed procedures are provided in the supplementary information (Appendix S1).

2.4. Selection and categorization of study

We checked the maximal BOLD response of each study to see whether there were iEEG electrodes within the region. Only the studies having an electrode within 2 cm of the peak voxel were included (Khoo et al., 2017). The distance of 2 cm was used since the electrode spacing is rarely less than 2 cm, making it the best precision we can get. Studies without electrodes in the maximal BOLD response were excluded due to inability of judging concordance between iEEG findings and BOLD results. According to the criteria described in a previous publication (Khoo et al., 2017), in the t-map resulting from an EEG/fMRI study, the relationship between clusters with the highest and second highest t-values t_1 and t_2 can reliably indicate concordance between the maximal BOLD and the seizure-onset zone (SOZ) as defined in a subsequent iEEG study. Classification analysis based on support vector machine was done using t_1 and t_2 as features. Let $x = |t_1|$, $y = (|t_1| - |t_2|)$, it was found that the value $z = 0.025x + 0.080y$, was a good variable to separate studies very likely to have concordant SOZ and maximal BOLD (Khoo et al., 2017). If the maximal BOLD response is highly significant (large value of t_1) and the second highest response is much less significant (t_2 much smaller than t_1) or there is no other significant response ($t_2 < 3.1$), it is very likely that the maximal BOLD response points to the SOZ. We selected the value $z > 0.4$ as indicating a first group of studies in which BOLD and SOZ were all concordant. For values of $z < 0.4$, some studies were concordant and some were discordant. We separated them into the concordant studies (group 2) and the discordant studies (group 3). The studies in these three groups were analyzed separately.

The SOZ was defined in the SEEG as the first change in the EEG leading to an unequivocal seizure discharge (Spanedda et al., 1997). Concordance between the maximum BOLD and the SOZ was present if the channel closest to the maximum BOLD (within 20 mm) was part of the SOZ.

2.5. Intracerebral EEG acquisition

Multi-contacts stereo-EEG electrodes (DIXI Medical, Besancon, France) were implanted using image-guided stereotaxy and set up as in previous studies (Olivier et al., 1994; Hall and Khoo, 2017). iEEGs were recorded using the Harmonie EEG system (Stellate, Montreal, Canada) at a sampling rate of 2000 Hz. iEEG data were analyzed using a bipolar montage between adjacent contacts on each electrode. Electro-oculographic–electromyographic and/or subdermal thin wire electrodes (Ives, 2005) were used, allowing identification of sleep stages.

2.6. Assessment of vigilance state during EEG-fMRI and selection of interictal iEEG recordings

Patient's vigilance state during EEG-fMRI were evaluated. For iEEG segments that fulfilled our inclusion criteria, their vigilance states were also evaluated. The first continuous 6-minute (matching the time length of each fMRI run) iEEG with IEDs in any channel and matching vigilance state was chosen for analysis. More details of the vigilance states evaluation and our inclusion criteria for iEEG are provided in supplementary information (Appendix S2).

2.7. Functional connectivity zone (Fig. 1A)

fMRI images preprocessing for functional connectivity analysis was done following the pipeline of previous study (Khoo et al., 2019). Details are provided in supplementary information (Appendix S3).

The maximal BOLD of different types of IEDs in each subject was analyzed separately. The voxel with maximal absolute t-value and its neighboring 26 voxels (voxels that are within one voxel diameter to the center voxel) was set as seed and its mean time series was computed to represent the activity of the region (Long et al., 2016; Liu et al., 2012). Pearson's correlation coefficients with this seed were calculated for all other voxels in the brain and the r-values were normalized using Fisher's transformation to derive the connectivity measure, resulting in a whole-brain functional connectivity map for each run. Second-level analysis was conducted for each study, on the connectivity matrices corresponding to the different runs, using a one-sample t-test. Significantly connected voxels were identified using an uncorrected $p < 0.001$ significance threshold and contiguous voxel size > 10. The Functional Connectivity Zone (FCZ) was defined as the set of all voxels with significant connectivity to the maximal BOLD seed. Additionally, the average connectivity of each voxel inside the FCZ across all runs was calculated for each study and back-transformed to r-value.

2.8. Localization and classification of iEEG channels (Fig. 1B)

Post-implantation MR or CT images were linearly co-registered to the preimplantation T1-weighted image using MINC tools (https://github.com/BIC-MNI). The trajectory and localization of each electrode was manually marked in the post-implantation MRI or CT. The coordinates of each electrode contact were computed from the distance between contacts and the coordinates of the entry and end points of the electrodes, using a visualization platform for neuro-navigation (IBIS) (Mercier et al., 2011). The coordinates of bipolar channels were computed as the midpoint of two adjacent contacts. We used SPM-12 (www.fil.ion.ucl.ac.uk/spm) to segment the preimplantation T1-weighted image and create a mask of cerebral cortex to exclude channels outside the brain. Channels were classified as inside or outside the FCZ, based on their location. Channels within 20 mm of the maximal BOLD voxel were excluded since at such a short distance volume conduction could affect EEG activity (Lachaux et al., 2003), masking the effect of the neuronal propagation that we aim to study.

2.9. IED detection in iEEG (Fig. 1C)

The large amount of iEEG data and channels makes manual detection of IEDs very time-consuming. Moreover, the inter-rater reliability among experts is highly variable (Gaspard et al., 2014), with a false detection rate that may disturb our analysis. Therefore, we adopted the

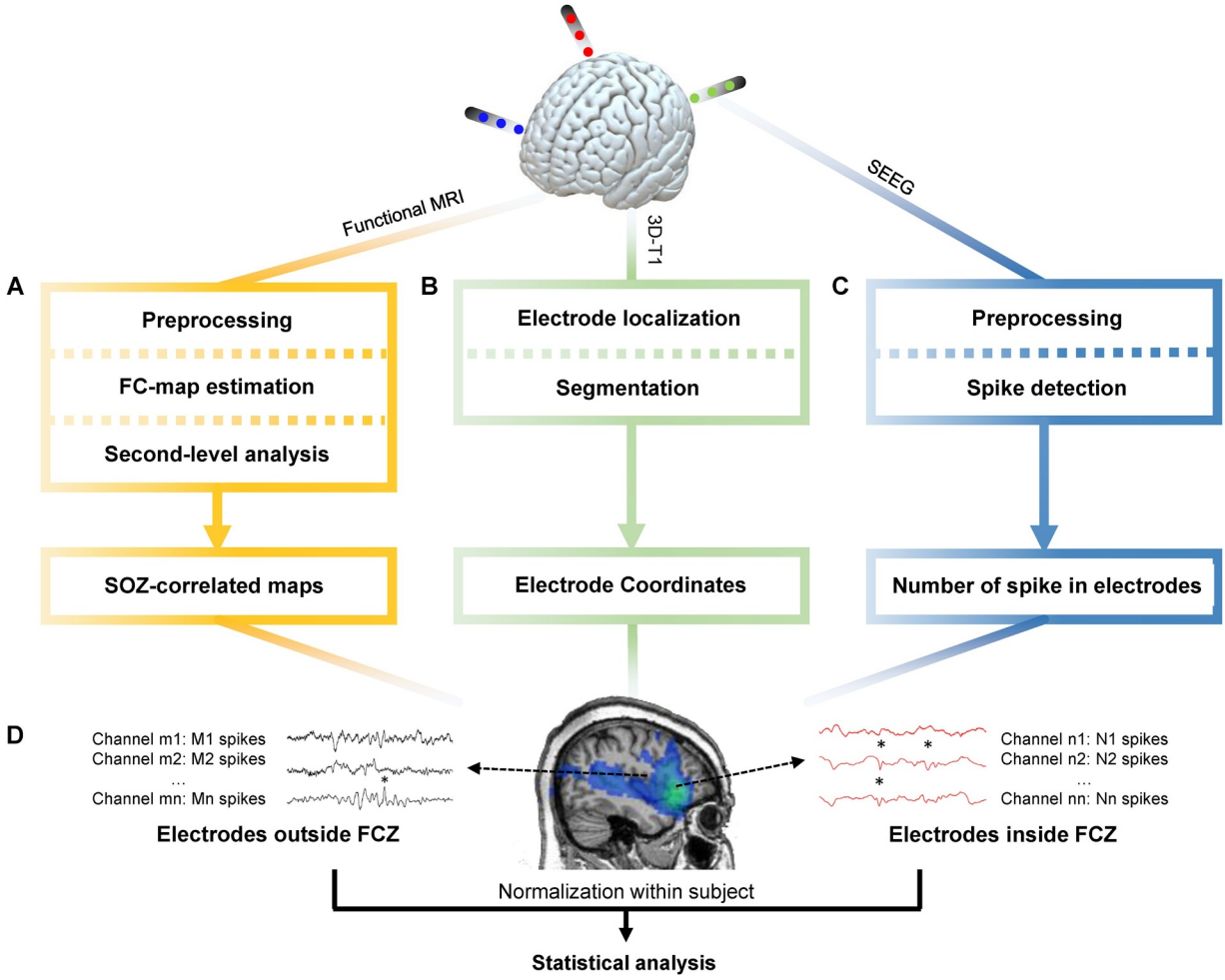

Fig. 1. General pipeline of the research.
(A) Functional MRI data was preprocessed through realignment, slice timing, outlier detection, coregistration, segmentation, spatial smoothing and noise regression. Then the maximal BOLD response and its neighbouring 26 voxels were used as seed regions to calculate the seed-based functional connectivity maps. One-sample *t*-test was applied to determine regions with significant functional connectivity. (B) Preimplantation 3D-T1 images were segmented to obtain the brain region. The postimplantation 3D-T1 images were first coregistered to the preimplantation images and then the location of electrodes were determined. (C) The iEEG data was resampled to 200 Hz, band-passed filtered between 10 and 60 Hz and notch filtered at 60 Hz to eliminate noise. Spike detection based on signal envelope distribution modelling was applied afterwards. (D) The number of IEDs in each channel was normalized by the median number of IEDs in each subject. Statistical analysis was performed to determine group difference of IED rates between channels inside and outside the FCZ.

automatic IED detection algorithm proposed by Janca et al. (Janca et al., 2015). The algorithm was validated and proved sensitive enough upon informal visual inspection, and it detects IEDs objectively and reproducibly (Ung et al., 2017).

Briefly, signals are down sampled to 200 Hz, followed by 10–60 Hz bandpass and 60 Hz notch filters. The signal envelope is calculated with the absolute value of the Hilbert transform. Moving windows of 5 s with 4 s overlap are used to model a log-normal statistical distribution of the signal envelope. A threshold of $\kappa_1 \times$ [Mode + Median] is applied for initial IED detection; the optimum κ_1 in the mentioned study is 3.65, determined empirically through cross-validation (Janca et al., 2015). Besides the original method, to eliminate false detections caused by bursts of rhythmic activity such as alpha activity, we set a rule that if 4 or more consecutive 120msec segments have probability above 90% of being classified as IEDs, they will be considered a burst of rhythmic activity and not labelled as IEDs.

The IED detection was repeated with parameter κ_1 varying between 3 and 4, in steps of 0.05, to ensure that results were not affected by detection sensitivity. A subset of candidate IEDs was randomly selected across all patients and visually validated by an expert to qualitatively confirm adequate performance.

2.10. Statistical analysis (Fig. 1D)

After IED detection, the IED rate at each channel was divided by the median IED rate in all channels of each subject to emphasize inter-regional rate differences rather than absolute differences. The IED rates in channels inside and outside the FCZ (i.e. in regions with or without significant connectivity to the maximal BOLD) were grouped, and a two-sample *t*-test was conducted to determine whether there was a difference in IED rates between channels inside and outside the FCZ in the three groups of studies. Effect size (Hedge's g) and degree of freedom (DOF) were calculated for better evaluation of the statistical analysis. We also conducted the two-sample Kolmogorov-Smirnov test (KS-test), a nonparametric statistical test in order to confirm our findings in the two-sample *t*-tests.

For verification, we randomly chose three seeds in the cerebral cortex, at least 20 mm away from the maximal BOLD seeds of all studies of each subject and outside the FCZ of each study. The corresponding seed-based functional connectivity maps were computed and the channels reclassified following the same procedure as for the maximal BOLD seed. Identical statistical analysis was done to compare IED rates inside and outside the FCZ based on the random seeds.

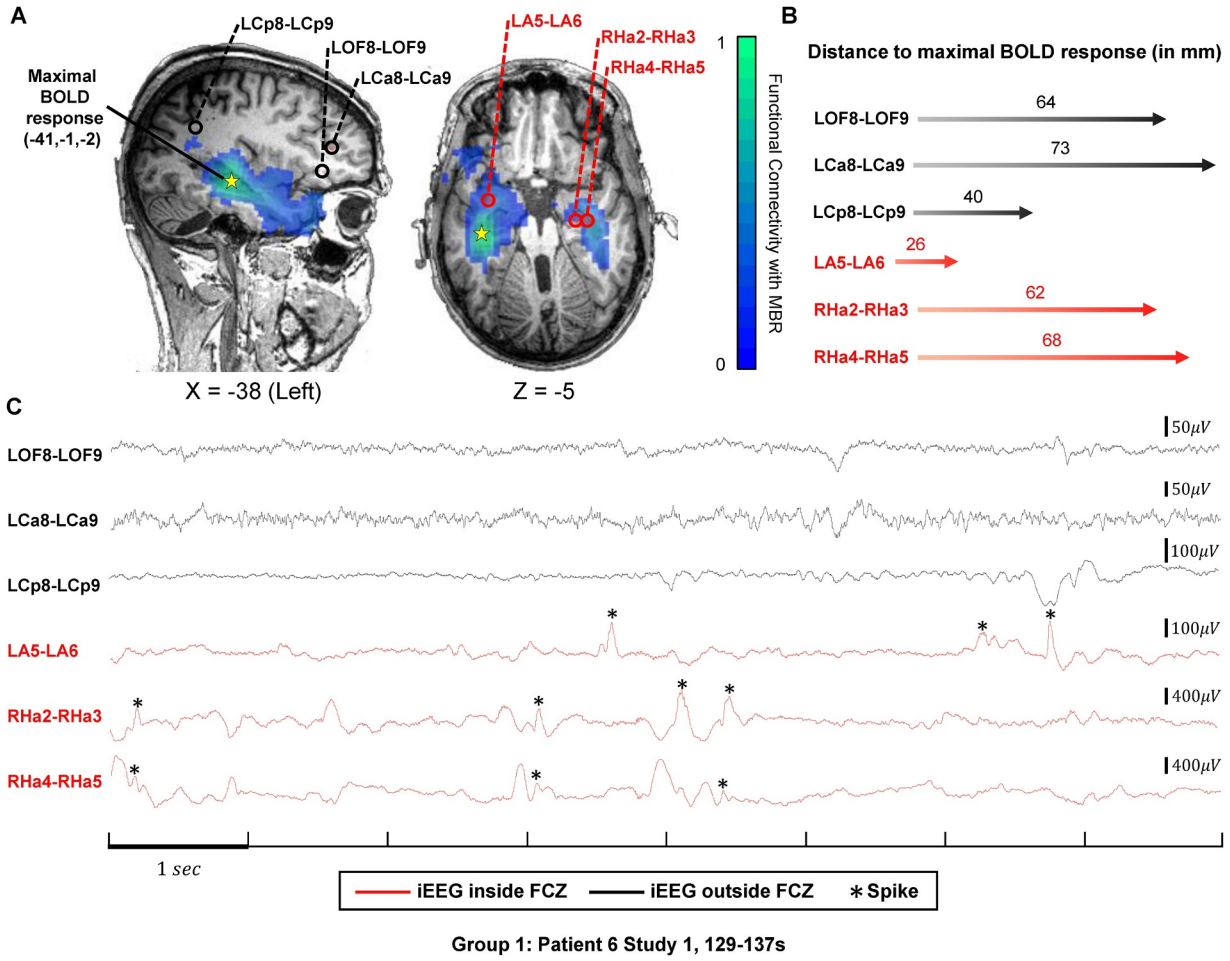

Fig. 2. IEDs in channels inside and outside the FCZ in Group 1.
(A) Functional connectivity map of the maximal BOLD response in green and blue according to the color bar. Three channels (LA5-LA6, RHa2-RHa3, RHa4-RHa5) inside the FCZ were selected in two orthogonal slices ($X = -38$, $Z = -5$). They are marked with red circles and names in red. Three channels (LOF8-LOF9, LCa8-LCa9, LCp8-LCp9) outside the FCZ are selected for comparison, labelled with black circle and names in black. The projection of maximal BOLD response in each slice is shown by the yellow star (MNI coordinate $(-41, -1, -2)$). (B) Distance between the above six channels and the maximal BOLD response in millimeter and illustrated by the length of the arrow. (C) Representative 8-second segment of the six channels. Channels inside the FCZ in red; channels outside in black. IEDs are denoted by asterisks. There are more IEDs in channels inside the FCZ than outside.

The Euclidean distance between iEEG channel and the maximal BOLD voxel could be a factor of importance in IED presence, i.e., channels close to the maximal BOLD may exhibit more IEDs purely as a function of distance and regardless of functional connectivity. The laterality between channels and the maximal BOLD response may also affect IED presence, i.e., channels in the same hemisphere as maximal BOLD may exhibit more IEDs. We used a two-sample *t*-test to determine if there was a difference in distance between the channels inside and outside the FCZ. Then the between-group difference in normalized IED rate was recalculated using the distance to the maximal BOLD and laterality factor as covariate. The normalized IED rate was regarded as explanatory variable while the distance and laterality factor as dependent variables. Linear regression was then applied and the residual was the regressed IED rate, thus eliminating the potential effects of distance and laterality.

2.11. Correlation analysis

For channels inside the FCZ, we calculated the Spearman's correlation coefficient between functional connectivity and the IED rate in the three groups to see if higher functional connectivity was related to higher IED rates. Here the functional connectivity of a channel was determined as the *r*-value of the voxel overlapping it.

2.12. Data availability

Anonymized data not published within this article will be available upon request for qualified investigators, under approval by the research ethics board of the Montreal Neurological Institute and Hospital.

3. Results

Among the 38 selected patients, 22 had one type of IED, 7 had two, 6 had three, and 3 had four, for a total of 66 IED-related studies. Sixteen studies without significant BOLD response in the gray matter and 10 without implantation in the maximal BOLD response were excluded. Two subjects were also excluded because they did not have an iEEG segment matching the vigilance state during the EEG/fMRI study. Hence, 37 studies from 25 patients were analyzed (clinical and electrophysiologic characteristics in Table S1). Seventeen studies were categorized in Group 1 (distinct peak BOLD i.e. $z > 0.04$ and SOZ concordance), 12 in Group 2 (SOZ concordance but less distinct peak BOLD i.e. $z \leq 0.04$) and 8 in Group 3 (discordant between SOZ and peak BOLD). The first and second studies in patient 3 of Group 2 had identical maximal BOLD peak voxel and were in the same group; we therefore excluded the second study with lower *t*-value. Eleven studies were left in Group 2.

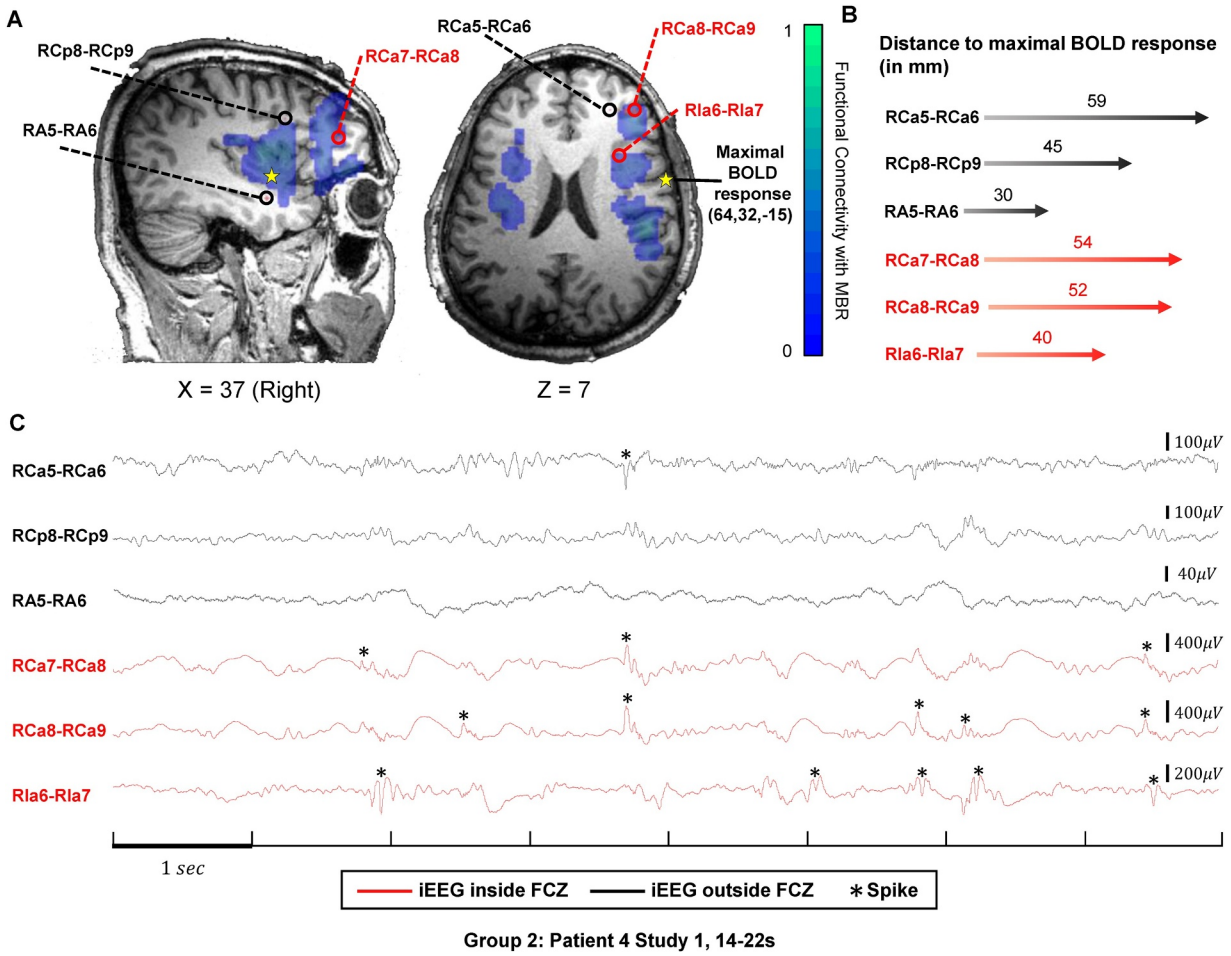

Fig. 3. IEDs in channels inside and outside the FCZ in Group 2.
(A) Functional connectivity map of maximal BOLD response in green and blue color according to the color bar. Three channels (RCa7-RCa8, RCa8-RCa9, RIa6-RIa7) inside the FCZ were selected in two orthogonal slices ($X = 37$, $Z = 7$). They are denoted with red circles and names in red. Three channels (RCa5-RCa6, RCp8-RCp9, RA5-RA6) outside the FCZ are selected for comparison, labelled with black circle and names in black. The projection of maximal BOLD response in each slice is shown by the yellow star (MNI coordinate (64,32, − 15)). (B) The distance between the above six channels and the maximal BOLD response in millimeter and illustrated by the length of the arrow. (C) Representative 8-second segment of the six channels. Channels inside the FCZ in red; channels outside in black. IEDs are denoted by asterisks. There are more IEDs in channels inside the FCZ than outside.

3.1. Functional connectivity analysis

The average duration of EEG/fMRI recording was 58.8 min (range, 30–90); thus approximately 10 functional connectivity matrices were calculated for each subject since a matrix was obtained for each 6-min run. After the second-level analysis across the runs, a mask of the FCZ and a mean functional connectivity map were generated for each study.Figs. 2–4 show that the FCZs distributed bilaterally and diffusely, showing widespread rather than focal characteristics.

3.2. Localization and classification of iEEG contacts

There was a total of 2385 contacts and an average of 95 contacts (range, 44–128) per subject. After excluding 117 contacts outside the cortex, we combined adjacent contacts to create bipolar montages, resulting in 1554 bipolar channels, with a median of 62 channels (range, 20–115) per subject. Five noisy channels with abnormal amplitude and waveform were removed in three subjects. In Group 1, 147 channels were excluded due to their close distance to the maximal BOLD voxel (< 20 mm), resulting in 358 channels inside and 553 outside the FCZ. In Group 2, 99 channels were excluded, resulting in 185 channels inside the FCZ and 596 outside. In Group 3, 33 channels were excluded, 67 channels were inside the FCZ and 490 were outside.

3.3. iEEG data and IED detection

Six-minute iEEG data was selected for each subject. By using the optimal IED detection parameter $\kappa_1 = 3.65$ (Janca et al., 2015), an average of 40 IEDs were detected in each channel (range, 0–553) in Group 1, 34 (range, 0–520) in Group 2 and 47 (range, 0–273) in Group 3. After normalization by the median IED rate of each subject, the average normalized IED rate was 1.8 (range, 0–46) in Group 1, 2.7 (range, 0–80) in Group 2 and 2.2 (range, 0–26) in Group 3. In Group 1, the normalized IED rate was 2.7 ± 2.5 in channels inside the FCZ and 1.3 ± 0.8 in channels outside the FCZ, in Group 2, 3.8 ± 3.7 and 2.3 ± 2.1, and in Group 3, 1.3 ± 0.8 and 2.3 ± 1.8. In Group 1, 12 out of 358 channels inside the FCZ and 74 out of 553 channels outside the FCZ did not show any IED. In Group 2, the numbers are 40 out of 268 and 94 out of 618. In Group 3, the numbers are 4 out of 84 and 71 out of 506. In Fig. 2 (example from Group 1), the normalized IED rates in channels within the FCZ are higher than that in channels outside the FCZ. In Fig. 3 (example from Group 2), channels inside the FCZ also have more IEDs than channels outside the FCZ. In Fig. 4 (example from Group 3), no difference in normalized IED rates can be seen between channels inside and outside the FCZ.

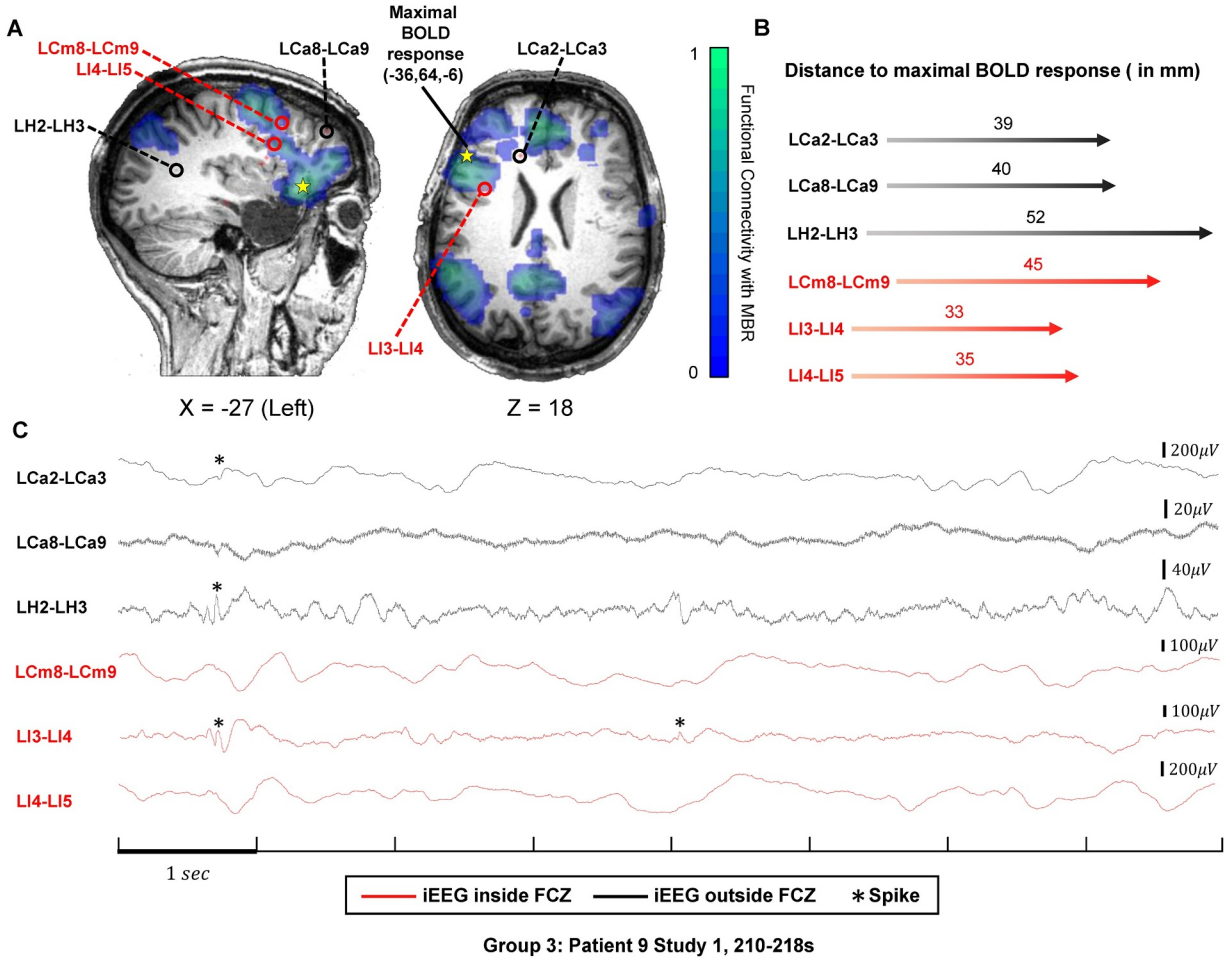

Fig. 4. IEDs in channels inside and outside the FCZ in Group 3.
(A) Functional connectivity map of maximal BOLD response in green and blue color according to the color bar. Three channels (LCm8-LCm9, LI3-LI4, LI4-LI5) inside the FCZ were selected in two orthogonal slices ($X = -27, Z = 18$). They are denoted with red circles and names in red. Three channels (LCa2-LCa3, LCa8-LCa9, LH2-LH3) outside the FCZ are selected for comparison, labelled with black circle and names in black. The projection of maximal BOLD response in each slice is shown by the yellow star (MNI coordinate (36,64, −6)). (B) The distance between the above six channels and the maximal BOLD response in millimeter and illustrated by the length of the arrow. (C) Representative 8-second segment of the six channels. Channels inside the FCZ in red and channels outside in black. IEDs are denoted by asterisks. IEDs occurred in channels both inside and outside the FCZ and the amount are almost the same.

3.4. Statistical analysis

We compared the IED rates between channels inside and outside the FCZ under the same IED detection parameter κ_1 using a right-tail (rates inside the FCZ > rates outside the FCZ) two-sample *t*-test. We used the optimum $\kappa_1 = 3.65$ first. In Group 1, the rates inside the FCZ were significantly larger than outside the FCZ (two-sample *t*-test: p-value = 2.6×10^{-6}, t-value = 4.60, effect size = 0.36, DOF = 762; KS-test: p-value = 4.2×10^{-6}, Fig. 5A). In Group 2, the inequality held with lower significance (two-sample *t*-test: p-value = 1.2×10^{-3}, t-value = 3.05, effect size = 0.26, DOF = 779; KS-test: p-value = 1.5×10^{-3}, Fig. 5B). In Group 3, no superiority in IED rates was seen in channels inside the FCZ compared to channels outside the FCZ (two-sample *t*-test: p-value = 0.97, t-value = −1.95, effect size = −0.25, DOF = 555; KS-test: p-value = 0.77, Fig. 5C). We then varied κ_1 from 3 to 4 in steps of 0.05 and the difference remained significant in Group 1 (maximal $p < 10^{-4}$) and Group 2 (maximal $p < 0.002$). The result for Group 3 held as well (minimal $p = 0.968$). If IED rates are averaged for each study to remove the effect of unequal number of channels across patients, inside and outside the FCZ, the difference between groups remains statistically significant (Group 1: $p = 0.026$; Group 2: $p = 0.057$; Group 3: $p = 0.99$).

For further verification, we randomly selected three seeds at least 20 mm away from the maximal BOLD voxel of all studies in each subject and applied the same analysis to examine the difference of IED rates under the optimal IED detection parameter $\kappa_1 = 3.65$. There was no significant difference in the IED rates inside and outside the zone functionally connected to the random seeds (for the three sets of random seeds we got $p = 0.25$, $p = 0.99$, $p = 0.21$; Fig. 6A-C).

We compared the Euclidian distance between channels and the maximal BOLD voxel and found a shorter distance for channels inside the FCZ compared to channels outside in all three groups ($p < 10^{-11}$, $p < 10^{-3}$, $p < 10^{-4}$ for Group 1, Group 2 and Group 3, respectively, Fig. 7A). To account for the effect of distance between channels and the maximal BOLD voxel as well as laterality, we regressed the distance and laterality factors out of the IED rates and compared the regressed[1] IED rates inside and outside the FCZ. The difference in the mean remained significant for Group 1 ($p = 1.5 \times 10^{-6}$ for the IED detection parameter $\kappa_1 = 3.65$ and $p < 4 \times 10^{-5}$ in the $3 < \kappa_1 < 4$ range) and Group 2 ($p = 0.013$ for the IED detection parameter $\kappa_1 = 3.65$ and $p < 0.017$ in the $3 < \kappa_1 < 4$ range). In Group 3, regressed IED rates in channels inside the FCZ were not larger than that of channels outside the FCZ

[1] The font size of different number are different. Please make sure it is in the same size.

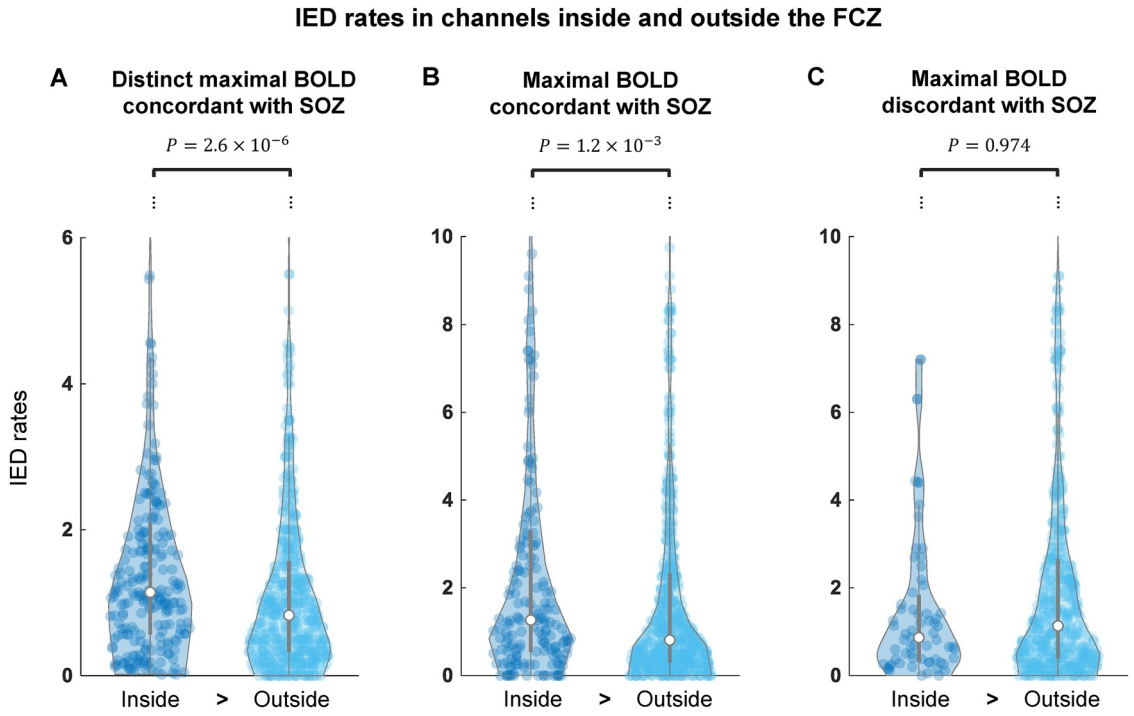

Fig. 5. Violin plots of IED rates in channels inside and outside FCZ.
Kernel density plot (shape), median (white circle), interquartile range (inner grey line), and all individual values of IED rates (colored circles). Parameter κ_1 for spike detection set to 3.65, the suggested optimum. Inequality signs in X-axis indicate right-tail two-sample *t*-test. (A) Patients in Group 1 have prominent maximal BOLD responses in EEG/fMRI analysis, concordant with SOZ. IED rates in channels inside the FCZ are significantly higher than those outside the FCZ ($p < 10^{-5}$); (B) Patients in Group 2 do not have maximal prominent BOLD responses but the maximal responses were also concordant with the SOZ. IED rates in channels inside the FCZ are also significantly higher than those outside the FCZ ($p = 0.001$); (C) The maximal BOLD responses in patients of Group 3 are discordant with the SOZ. IED rates in channels inside the FCZ are not higher than channels outside the FCZ ($p = 0.974$).

($p > 0.994$ in the $3 < \kappa_1 < 4$ range). The results after regression of distance are shown in Fig. 7B.

3.5. Correlation analysis

There was a significant correlation between IED rates and the average functional connectivity value at the location of the channels in the FCZ in Group 1 (Spearman's correlation coefficient $r = 0.13$, $p < 0.05$, Fig. 8A), while in Group 2 (Spearman's correlation coefficient $r = 0.13$, $p = 0.09$, Fig. 8B) and Group 3 (Spearman's correlation coefficient $r = 0.09$, $p = 0.47$, Fig. 8C) this correlation was not significant.

4. Discussion

Functional connectivity as measured by resting state fMRI is a reliable and effective metric to determine functional coordination and interaction between different brain regions (Greicius et al., 2003; Solomon et al., 2018). In the present study we compared fMRI responses related to scalp IEDs to subsequent iEEG investigations. We found that, in fMRI studies having maximal BOLD response concordant with iEEG-defined SOZ, iEEG channels in the regions functionally connected to the maximal BOLD have higher IED rates than channels outside the functionally connected regions. Among these studies, those with a distinct, relatively isolated maximal BOLD response show a correlation between IED rates and functional connectivity strength. Our findings suggest that fMRI connectivity is a marker of the spatial distribution of IEDs and can reveal, non-invasively, the brain regions where IEDs are likely to be present in a subsequent invasive iEEG study.

In a previous study, we examined the relationship between iEEG activity and the different BOLD clusters of the t-map from the EEG/fMRI analysis (Khoo et al., 2017). Only t-maps with more than one activation cluster were studied, focusing on regions that were active at the time of scalp IEDs and reflecting intracranial events widespread enough to be seen on the scalp. However, in iEEG, there are locally generated interictal activities not strong or spatially extended enough to be seen on the scalp. This local activity could still be reflected in the BOLD signal (Khoo et al., 2017), or indirectly as ongoing functional connectivity that parallels the spiking distribution, as we demonstrate in this study. In this situation, functional connectivity analysis could predict the regions involved in spiking.

Several studies have investigated epileptic networks through resting state fMRI analysis (Lee et al., 2018; Dansereau et al., 2014; Pittau et al., 2012). The present study uses a different approach to find epileptic networks, performing a seed-based analysis with a seed selected in the core of the network. Other seeds such as EEG or MEG sources or MRI lesions could be considered as well.

We used IED rates as measures of whether a region is in an epileptic network instead of the more commonly used correlation between channels showing epileptic discharges (Khoo et al., 2017; Khoo et al., 2019). A correlation measure or similar EEG functional connectivity metric might not account for interictal activity propagating with long latency. Moreover, secondary epileptogenic zones that also generate IEDs (Scholly et al., 2013) under the indirect influence of the focus, may result in low functional connectivity with the network core because their IEDs are not time-locked with that of the core. Our focus is on the relationship between BOLD functional connectivity and the intensity of iEEG interictal activity. The IED rate objectively reflects the amount of interictal activity in each channel, regardless of any time delay or effect of secondary sources, making it a suitable choice for our study.

A correlation was found between strength of fMRI connectivity and IED rate in channels inside the FCZ in Group 1 but not in Group 2. This indicates that a distinct and concordant maximal BOLD response in EEG/fMRI may represent a clear and “dominant” epileptic focus from

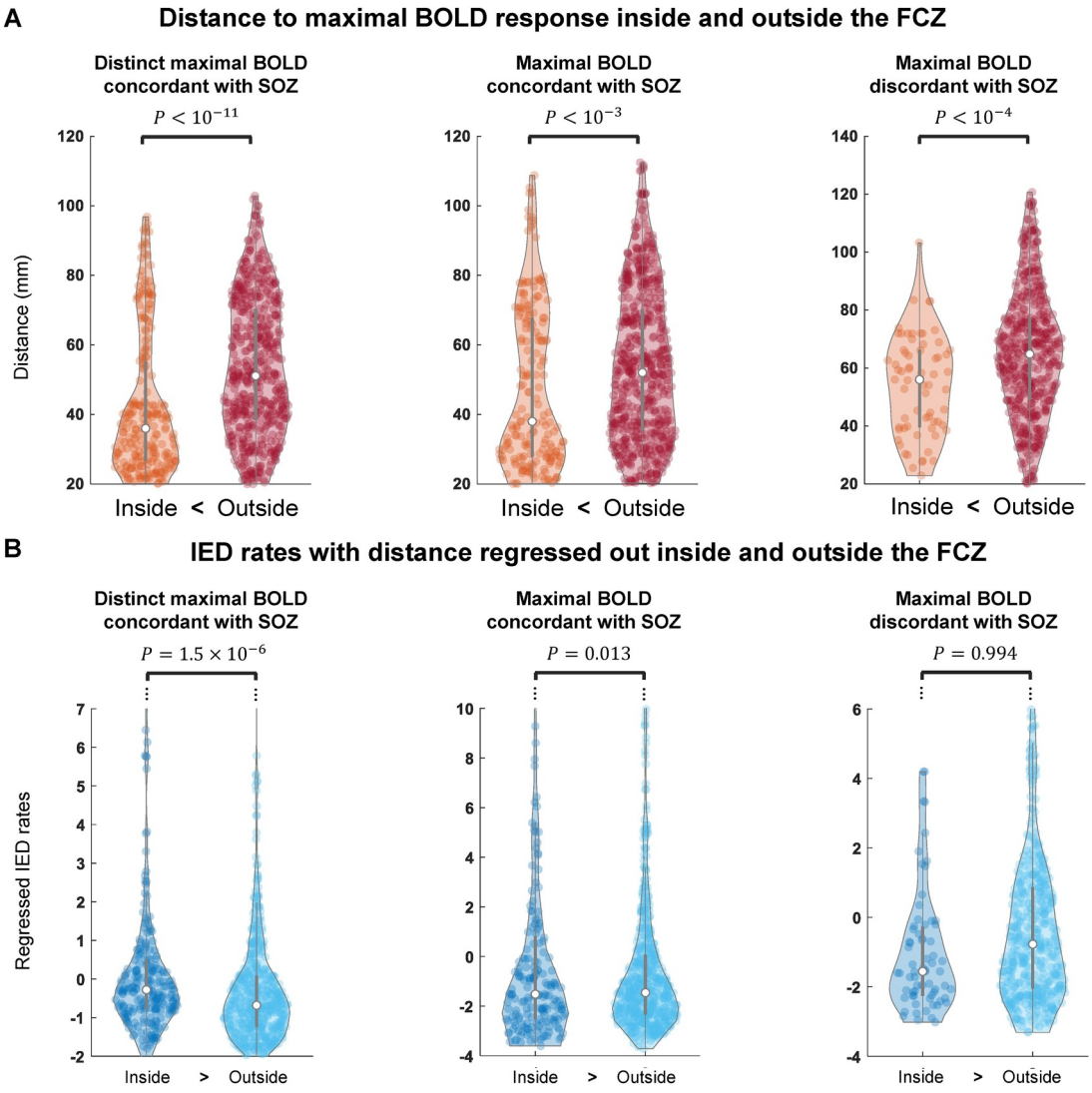

Fig. 6. IED rates in channels inside and outside of FCZ in the random seed test.
Parameter κ_1 for spike detection set to 3.65, the suggested optimum. Inequality signs in the X-axis indicate right-tail two-sample *t*-test. Kernel density plot (shape), median (white circle), interquartile range (inner grey line), and all individual values of IED rates (colored circles). (A) In the first (A), second (B) and third (C) random seed tests, IED rates in channels inside the FCZ are no larger than outside ($p = 0.25$, $p = 0.99$, $p = 0.21$, respectively).

which epileptic activity spreads. Therefore, the functional connectivity between this focus and other brain regions may be able to delineate with some precision the interictal epileptic network. Although concordant with the SOZ, a less distinct maximal BOLD (our Group 2 with $z \leq 0.4$) may represent a more complex pattern of the epileptic discharges that are not as fully determined by the activity of the maximal BOLD. For instance, there may be intrinsic epileptogenicity outside the maximal BOLD, where the influence of the region of maximal BOLD is weak.

One may ask whether the functional connectivity can be dominated by the response to scalp IEDs, rendering the functional connectivity zone similar to the BOLD response zone. We estimated the amount of time during which the BOLD signals may be affected by scalp IEDs and the percentage is 19.5%. Therefore, the functional connectivity maps in our analysis are mainly dependent on the background BOLD signal rather than on the presence of IEDs.

Physical distance away from the peak BOLD and laterality did not have an effect in our results; the influence of the region of maximal BOLD over functionally connected regions occurs through neuronal pathways relatively independently of distance and laterality. This applies to regions not immediately around the maximal BOLD since previous studies hypothesized that within a short distance to the source of a discharge, the amplitude of the discharge decreases as the inverse square of the distance from the source, reflecting volume conduction (Ruch et al., 1965; Zaveri et al., 2009). Although validation showed that the decrease does not obey the rule strictly (Schevon et al., 2010), distance was suggested to be influential only in a close neighborhood. Since we selected channels a relatively long distance from the peak BOLD voxel (> 20 mm), the effects of volume conduction appear negligible. As for laterality, since the FCZ of all the studies involved both hemispheres with high symmetry, it is not surprising that channels inside and outside the FCZ were also distributed in a similar way. Therefore, laterality should not be a decisive factor of IED rates.

EEG/fMRI studies were correlated with the iEEG-defined SOZ and separated in three groups. If we use the non-invasive EEG/fMRI analysis alone (without knowing the iEEG-defined SOZ), EEG-fMRI studies can be separated in two groups: those with a distinct maximal BOLD response and those without a distinct response. We suggest that for the studies with a distinct BOLD response, most iEEG channels inside the FCZ exhibited IEDs and our non-invasive functional connectivity method can indicate brain regions that are likely to have high IED rates in iEEG, which could help to plan iEEG electrode implantation.

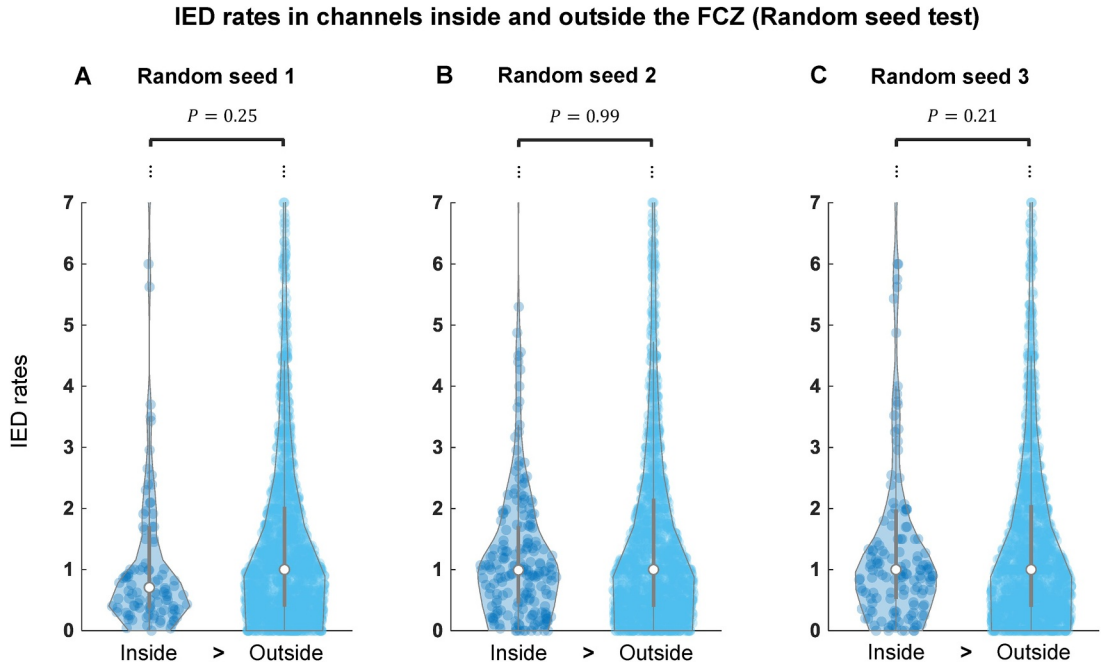

Fig. 7. Distance between iEEG channels and maximal BOLD and IED rates after regressing distance and laterality.
Kernel density plot (shape), median (white circle), interquartile range (inner grey line), and all individual values (distance in A, and regressed IED rates in B, colored circles). Parameter κ_1 for spike detection is set to 3.65, the suggested optimum. (A) In all three group of patients, distance to maximal BOLD response was significantly smaller in channels inside the FCZ than outside. ($p < 10^{-11}$, $p < 10^{-3}$, $p < 10^{-4}$, respectively). Inequality signs in the X-axis indicate left-tail two-sample *t*-test; (B) Distance and laterality are regressed from the IED rates and results of statistical analysis are consistent with Fig. 5. In Groups 1 and 2, regressed IED rates in channels inside the FCZ are significantly higher than outside. ($p = 1.5 \times 10^{-6}$, $p = 0.013$ respectively). In Group 3, IED rates in channels inside the FCZ are no higher than outside ($p = 0.995$). Inequality signs in the X-axis indicate right-tail two-sample *t*-test.

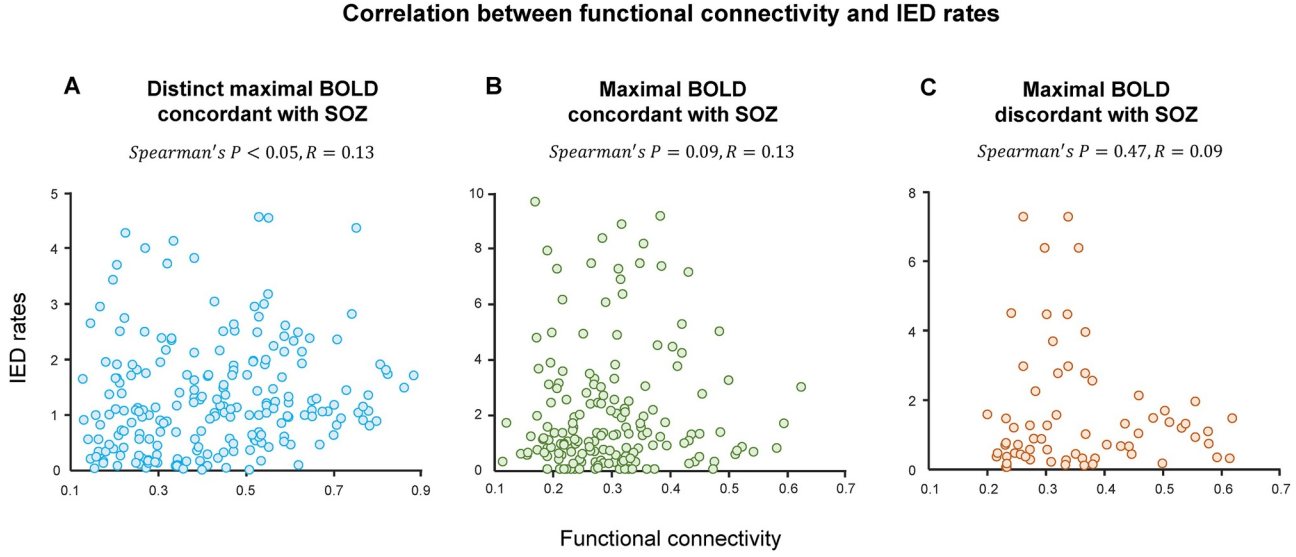

Fig. 8. Scatter plots of functional connectivity and IED rates in channels inside the FCZ.
The correlation was estimated using all the data while some outliers with high IED rates are not shown for better view. (A) In Group 1, IED rates in channels inside the FCZ are correlated with functional connectivity (*Spearman's* $p < 10^{-5}$, $R = 0.13$); (B) In Group 2, IED rates in channels inside the FCZ have a tendency of linear correlation with functional connectivity (*Spearman's* $p = 0.09$, $R = 0.13$); (C) In Group 3, IED rates in channels inside the FCZ show no linear correlation with functional connectivity (*Spearman's* $p = 0.974$, $R = 0.09$). Parameter κ_1 for spike detection is set to 3.65, the suggested optimum.

5. Methodological considerations and future research

As with any iEEG study, spatial sampling is limited. However, in all studies there were channels inside and outside the FCZ. The fMRI and iEEG were not carried out simultaneously but we nevertheless found statistically significant difference in this situation, pointing to a robust relationship between functional connectivity and IED rates. This relationship might be stronger if the studies had been done simultaneously.

We did not evaluate the latency between IEDs, which may better describe the propagation of IEDs (Khoo et al., 2017). Since we were evaluating interictal activity across the whole brain, including regions highly correlated with the network core (maximum BOLD) and regions unrelated to this core, latency could not be computed in channels without IEDs. In contrast, the IED rate can be obtained in all channels, which allowed answering our research question.

Funding sources

This study is funded by Canadian Institutes of Health Research (FDN 143208) and the National Natural Science Foundation of China (61722313, and 61420106001), the National Key Research and Development Program (2018YFB1305101)

Declaration of Competing Interest

None.

Supplementary materials

Supplementary material associated with this article can be found, in the online version, at doi:10.1016/j.nicl.2019.102038.

References

An, D., Fahoum, F., Hall, J., Olivier, A., Gotman, J., Dubeau, F., 2013. Electroencephalography/functional magnetic resonance imaging responses help predict surgical outcome in focal epilepsy. Epilepsia 54, 2184–2194.

Bettus, G., Ranjeva, J.-P., Wendling, F., et al., 2011. Interictal functional connectivity of human epileptic networks assessed by intracerebral eeg and bold signal fluctuations. PLoS ONE 6, e20071.

Chauvière, L., Doublet, T., Ghestem, A., et al., 2012. Changes in interictal spike features precede the onset of temporal lobe epilepsy. Ann. Neurol. 71, 805–814.

Coutin-Churchman, P.E., Wu, J.Y., Chen, L.L.K., Shattuck, K., Dewar, S., Nuwer, M.R., 2012. Quantification and localization of EEG interictal spike activity in patients with surgically removed epileptogenic foci. Clin. Neurophysiol. 123, 471–485.

Dansereau, C.L., Bellec, P., Lee, K., Pittau, F., Gotman, J., Grova, C., 2014. Detection of abnormal resting-state networks in individual patients suffering from focal epilepsy: an initial step toward individual connectivity assessment. Front. Neurosci-Switz 8, 419.

Foster Brett, L., Rangarajan, V., Shirer William, R., Parvizi, J., 2015. Intrinsic and task-dependent coupling of neuronal population activity in human parietal cortex. Neuron 86, 578–590.

Gaspard, N., Alkawadri, R., Farooque, P., Goncharova, I.I., Zaveri, H.P., 2014. Automatic detection of prominent interictal spikes in intracranial EEG: validation of an algorithm and relationsip to the seizure onset zone. Clin. Neurophysiol. 125, 1095–1103.

Greicius, M.D., Krasnow, B., Reiss, A.L., Menon, V., 2003. Functional connectivity in the resting brain: a network analysis of the default mode hypothesis. Proc. Natl. Acad. Sci. 100, 253.

Greiner, H.M., Horn, P.S., Tenney, J.R., et al., 2016. Preresection intraoperative electrocorticography (ECoG) abnormalities predict seizure-onset zone and outcome in pediatric epilepsy surgery. Epilepsia 57, 582–589.

Hall, J.A., Khoo, H.M., 2017. Robotic-Assisted and image-guided MRI-Compatible stereoelectroencephalography. Can. J. Neurol. Sci. / Journal Canadien des Sciences Neurologiques 45, 35–43.

Ives, J.R., 2005. New chronic EEG electrode for critical/intensive care unit monitoring. J. Clin. Neurophysiol. 22, 119–123.

Janca, R., Jezdik, P., Cmejla, R., et al., 2015. Detection of interictal epileptiform discharges using signal envelope distribution modelling: application to epileptic and non-epileptic intracranial recordings. Brain Topogr. 28, 172–183.

Khoo, H.M., Hao, Y., Ellenrieder, N., et al., 2017a. The hemodynamic response to interictal epileptic discharges localizes the seizure-onset zone. Epilepsia 58, 811–823.

Khoo, H.M., von Ellenrieder, N., Zazubovits, N., Dubeau, F., Gotman, J., 2017b. Epileptic networks in action: synchrony between distant hemodynamic responses. Ann. Neurol. 82, 57–66.

Khoo, H.M., von Ellenrieder, N., Zazubovits, N., Hall, J.A., Dubeau, F., Gotman, J., 2019. Internodular functional connectivity in heterotopia-related epilepsy. Ann. Clin. Transl. Neurol. 6, 1010–1023.

Khoo, H.M., von Ellenrieder, N., Zazubovits, N., He, D., Dubeau, F., Gotman, J., 2018. The spike onset zone: the region where epileptic spikes start and from where they propagate. Neurology.

Kucyi, A., Schrouff, J., Bickel, S., Foster, B.L., Shine, J.M., Parvizi, J., 2018. Intracranial electrophysiology reveals reproducible intrinsic functional connectivity within human brain networks. J. Neurosci. 38, 4230.

Lachaux, J.P., Rudrauf, D., Kahane, P., 2003. Intracranial eeg and human brain mapping. J. Physiol-Paris 97, 613–628.

Lee, K., Khoo, H.M., Lina, J.-M., Dubeau, F., Gotman, J., Grova, C., 2018. Disruption, emergence and lateralization of brain network hubs in mesial temporal lobe epilepsy. NeuroImage 20, 71–84.

Liu, L., Zeng, L.-L., Li, Y., et al., 2012. Altered cerebellar functional connectivity with intrinsic connectivity networks in adults with major depressive disorder. PLoS ONE 7, e39516.

Long, L., Zeng, L.L., Song, Y., et al., 2016. Altered cerebellar-cerebral functional connectivity in benign adult familial myoclonic epilepsy. Epilepsia 57, 941–948.

Marsh, E.D., Peltzer, B., Brown Iii, M.W., et al., 2010. Interictal eeg spikes identify the region of electrographic seizure onset in some, but not all, pediatric epilepsy patients. Epilepsia 51, 592–601.

Mercier, L., Del Maestro, R.F., Petrecca, K., et al., 2011. New prototype neuronavigation system based on preoperative imaging and intraoperative freehand ultrasound: system description and validation. Int. J. Comput. Assist. Radiol. Surg. 6, 507–522.

Moeller, F., Tyvaert, L., Nguyen, D.K., et al., 2009. EEG-fMRI: adding to standard evaluations of patients with nonlesional frontal lobe epilepsy. Neurology 73, 2023.

Olivier, A., Germano, I.M., Cukiert, A., Peters, T., 1994. Frameless stereotaxy for surgery of the epilepsies: preliminary experience. J. Neurosurg. 81, 629–633.

Pittau, F., Fahoum, F., Zelmann, R., Dubeau, F., Gotman, J., 2013. Negative bold response to interictal epileptic discharges in focal epilepsy. Brain Topogr. 26, 627–640.

Pittau, F., Grova, C., Moeller, F., Dubeau, F., Gotman, J., 2012. Patterns of altered functional connectivity in mesial temporal lobe epilepsy. Epilepsia 53, 1013–1023.

Ruch, T., Patton, H.D., Woodbury, J.W., Towe, A.L., 1965. Neurophysiology: W. B. Saunders Company.

Sabolek, H.R., Swiercz, W.B., Lillis, K.P., et al., 2012. A candidate mechanism underlying the variance of interictal spike propagation. J. Neurosci. 32, 3009.

Schevon, C.A., Goodman, R.R., McKhann Jr., G., Emerson, R.G., 2010. Propagation of epileptiform activity on a submillimeter scale. J. Clin. Neurophysiol. 27, 406–411.

Scholly, J., Valenti, M.-P., Staack, A.M., et al., 2013. Hypothalamic hamartoma: is the epileptogenic zone always hypothalamic? Arguments for independent (third stage) secondary epileptogenesis. Epilepsia 54, 123–128.

Smith, E.H., Schevon, C.A., 2016. Toward a mechanistic understanding of epileptic networks. Curr. Neurol. Neurosci. 16, 97.

Solomon, E.A., Kragel, J.E., Gross, R., et al., 2018. Medial temporal lobe functional connectivity predicts stimulation-induced theta power. Nat. Commun. 9, 4437.

Spanedda, F., Cendes, F., Gotman, J., 1997. Relations between eeg seizure morphology, interhemispheric spread, and mesial temporal atrophy in bitemporal epilepsy. Epilepsia 38, 1300–1314.

Staley, K., Hellier, J.L., Dudek, F.E., 2005. Do interictal spikes drive epileptogenesis? Neuroscientist 11, 272–276.

Staley, K.J., White, A., Dudek, F.E., 2011. Interictal spikes: harbingers or causes of epilepsy? Neurosci. Lett. 497, 247–250.

Ung, H., Cazares, C., Nanivadekar, A., et al., 2017. Interictal epileptiform activity outside the seizure onset zone impacts cognition. Brain 140, 2157–2168.

Zaveri, H.P., Duckrow, R.B., Spencer, S.S., 2009. Concerning the observation of an electrical potential at a distance from an intracranial electrode contact. Clin. Neurophysiol. 120, 1873–1875.